# A Low Cost Power Efficient Wireless Soil Moisture Sensor Network for Forest Ecosystem Monitoring

Thayer Whitney, Tori Nicholas, Sonia Naderi, Ali Abedi University of Maine, Orono, ME, USA thayer.whitney@maine.edu

Abstract—Forest ecosystem monitoring with high spatiotemporal resolution is of paramount importance for development of accurate prediction models. Current systems are bulky, use high power, and are costly to build and maintain. In this paper a novel low cost and power efficient wireless sensor network for soil moisture monitoring is proposed. This system is power efficient and low cost to enable wide spread monitoring. The proposed system was built by undergraduate students at UMaine's WiSe-Net lab under supervision of graduate students.

Index Terms—Wireless, sensors, networks, soil moisture, forest models.

#### I. Introductions

The quantity of water contained in a material like soil is called water content and this concept has been recently used in a variety of scientific as well as technical areas. Water content can be represented as ratio and its range can be between zero which represents completely dry to the value of saturation of material. Water content can be based on mass or volumetric and can be measured by soil moisture sensors. The standard way to determine soil moisture is called thermogravimetric method which is introduced in [1]. In this method, the weight loss of soil is measured after oven drying of soil with known volume at 105° C. The main issue with this method is that it is very time consuming to do this procedure and these measurements can not be repeated because of the destructive effects that can be caused to the soil. Recently, these destructive methods have been replaced by electronic sensors such as capacitance, impedance, dielectric and time domain reflectometer sensors [2]. Different soil moisture measurement techniques have been proposed in literature [3]-[5]. For instance in [5], authors proposed a way for measuring soil moisture content by monitoring soil electromagnetic radiation which depends on sensitivity of microwaves to soil moisture. Measuring electrical resistance of soil is one of the technologies that can be used in soil moisture sensors which can be done by inserting two separate rods into the soil which act a sensor [6]. This method is based on changing the soil conductivity by changing the water content of the soil. Frequency domain sensors has been proposed in [7]. These kind of soil moisture sensors measure soil impedance changes because of the water content variations. These sensors are available as single and multi sensor probes which offer different measuring techniques [8],

[9]. Recent techniques in measuring soil moisture are fiber optic sensors [10], [11], dye doped plastic fibers [12] and ceramic sensors [13]. These types of sensors are not very reliable and they are expensive. Authors in [14] proposed neutron scattering method for soil moisture monitoring which is not applicable from practical point of view.

This project is financially sponsored by National Science Foundation (NSF) grant #1920908.

978-1-5386-5541-2/18/\$31.00 ©2018 IEEE

In this project, we aim to develop a micro-controller based low cost soil moisture monitoring system that can track the soil moisture at different locations of the forest floor in real time to provide accurate data for enhancing the prediction models. The sensors take the moisture value and provide this input to the micro-controller for digitizing, coding, compression, and transmission using the on-board radio. Power is provided through a rechargeable battery with solar panels.

The rest of this paper is organized as follows. The network design is presented in section II following power system in section III. The paper is concluded in section IV.

## II. NETWORK DESIGN

## A. Nodes configuration

There are various network configurations that can be used for wireless sensing. Depending on the application scenario and data flow, a mesh, star, tandem, or ring configurations may be selected. The proposed network in this project is a star network configured to a non-beacon operation noting the data flow and need for power savings. This operational mode functions by placing the central coordinator node in an always ready mode. When a sensor node activates, a beacon request is transmitted from the sensor node to the central coordinator. The central coordinator responds with a beacon, allowing the sensor node to request association. Once this is acknowledged, the sensor node is able to transmit its data. This is acknowledged by the central collector. The sensor node then powers off to preserve power, or it may receive another association request from the central coordinator to maintain its connection to the network. This mode of operation places control of the transmission with the sensor node, rather than central collector node. Since the sensor node is most limited by the available power, this allows for the longest operation.

## B. Experimental Performance Measurements

The performance of any wireless link can be measured by looking at packet loss over various distances. This is vital in determining the maximum potential sensor node resolution, which is function of the range. Two sensor nodes were used in this experimental test. First node was connected to a laptop acting as base station receiving data from the other node which is acting as sensor. Received signal strength indicator (RSSI) and packet loss was measured at different distances. The sensor node was configured to send 100 packets of random characters at the desired center frequencies of 915 MHz. Once the transmission was complete, the second board was moved back to another distance (10, 50, 100, 150, 200, 250, and 300 ft) and transmission was repeated. These tests where also coupled with a review of the manufactures test data, with particular interest given to the directivity of the antenna, as well as the efficiency [15].

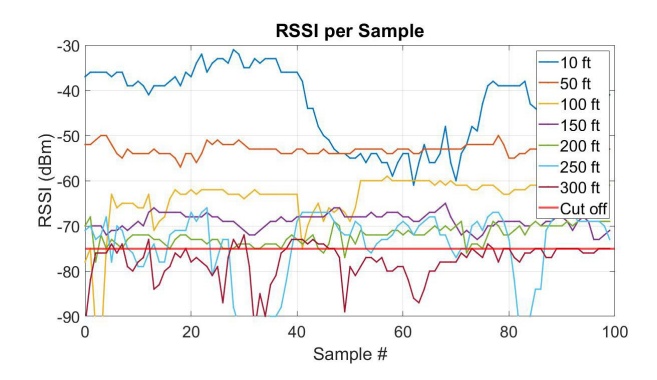


Fig. 1. RSSI at different distances with board antenna.

The first antenna tested, results shown above, was the antenna already included on the TI launchpad. Review of the manufacturer data showed a directivity of 4.61dBi, and an efficiency of 43.27%

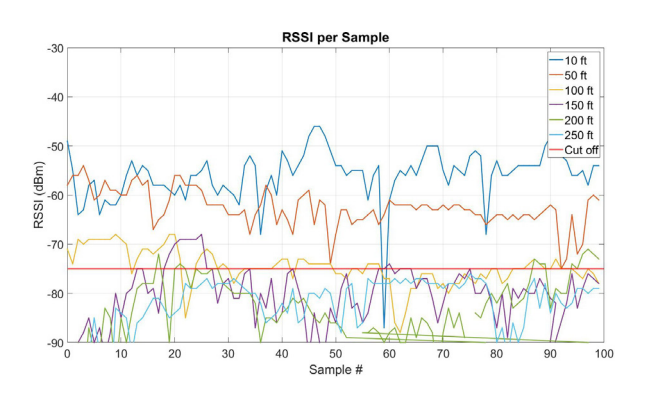


Fig. 2. RSSI at different distances with antenna 1

Antenna 1 was a CR2032 PCB Antenna [16], with an overall poor performance. It was the only antenna that the 300 ft tests results were not displayed, as there was such a significant gap in the test data due to poor transmission, that it was irrelevant to include in this report. Review of the manufacturer data showed a directivity of 4.25dBi, with an efficiency of 51.69% [17].

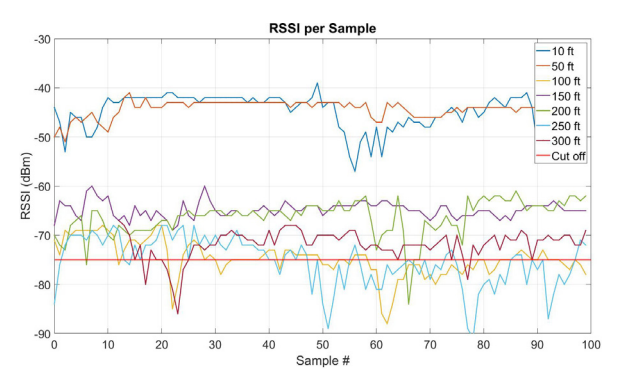


Fig. 3. RSSI at different distances with antenna 2

Antenna 2, a chip antenna from Fractus Antennas<sup>TM</sup> [16], preformed adequately. The manufacturer data was reviewed, and showed a directivity of 3.92dBi with an efficiency of 46.61% [17].

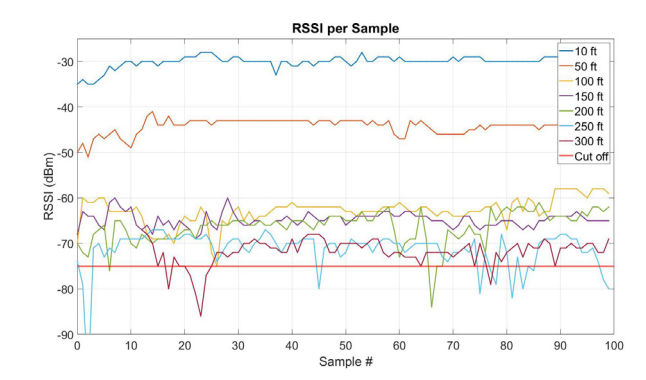


Fig. 4. RSSI at different distances with antenna 3

Antenna 3, a Compact PCB Helical Antenna [16], was the best preforming, showing the best potential to extend beyond the 300 ft range. Further review of the manufacturer data showed a directivity of 4.13 dBi, with an efficiency of 63.05% [17].

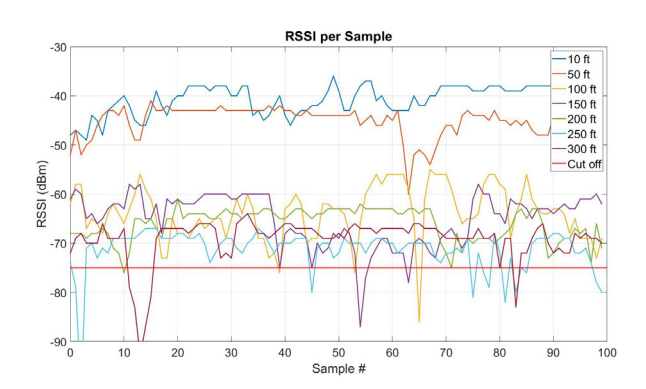


Fig. 5. RSSI at different distances with antenna 4

Antenna 4 was an array of two helical antennas placed orthogonal to each other for antenna diversity. It preformed similarly to antenna 3, and also provided a possibility for an extension in range. The manufacturer's test data showed a directivity of 4.39dBi, with an efficiency of 31.33% [17].

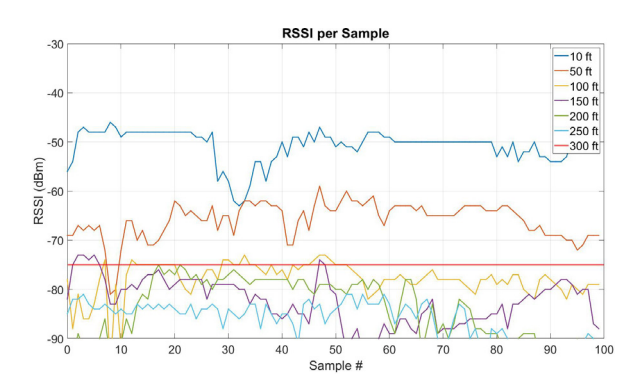


Fig. 6. RSSI at different distances with antenna 5

Antenna 5 was a PCB helical antenna. The worst performing, not quite reaching a 100 feet before falling below a level that was barely readable. Review of the manufacturer data gave a directivity of 4.16dBi, with an efficiency of 46.83%.

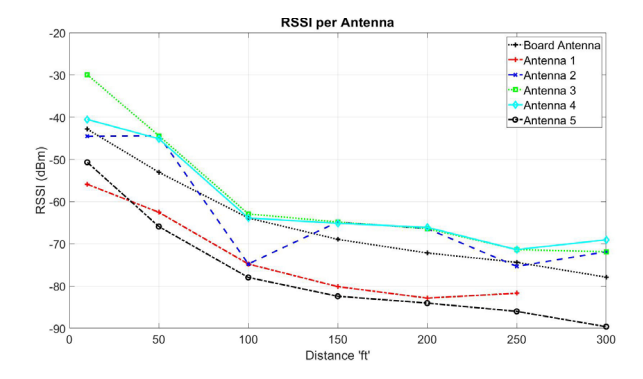


Fig. 7. RSSI of each antenna at each distance measured

The best preforming antennas where antenna 3 and 4, with the built in board antenna coming along closely behind. Using a RSSI cut off value of -75dBm, the built in antenna achieved a working distance of 250 ft, and for now, we will use the 250 ft. result to design our network grid. However, the compact PCB helical demonstrated in antenna 3 will be implement to increase the 250 ft. range. The overall footprint of antenna 3 was smaller also compared to the built-in antenna, allowing for a more compact device in the future. Additionally, there is 19.78% in efficiency between the built-in antenna and antenna 3. Since the largest consumption of power in this device is from the transmissions, any improvements in this area would provide substantial impact to the length of operation and range of the device.

## III. POWER SYSTEM

The power system for this project will consist of several subsystems to control the current and voltage of the incoming energy from solar panels and charge batteries efficiently. Block diagram of the power system is presented in figure 8.



Fig. 8. Block Diagram of the Power System

This block diagram shows the flow of power from the solar panel to the sensor node, which will power and read data from the sensors as well as communicate with other nodes to transmit the recorded data.

The power system needed to be low cost, powerful enough to provide long term continued operation, and not be so large as to make deployment and management of the system overly difficult. The component that provided the most difficulty in all of these categories was the battery.

## A. Battery Selection

Several different battery options were considered, ranging in chemistry, form factor, and availability. More mature battery technology, such as lead acid, nickel-metal hydride, and nickel-metal cadmium were all considered. However, all presented concerns with size and weight, complex charging algorithms, operational lifespan, as well ecological concerns. Lithium ion was eventually the chosen chemistry, for it high energy density, simpler charging algorithm, and operational lifespan. Using data from both laboratory measurements and the appropriate data sheets, an appropriate capacity was determined.

# $Avg.draw = Active draw \times %time active$

# + idle draw × % time idle

A minimum capacity of 1000mAh was then determined, using 2 weeks as the length of time that the device would be able to run solely on battery power, with no input from the solar array.

With the battery chemistry and capacity determined, two 18650 form factor batteries where chosen. These cylindrical cells, commonly found in portable power tools, power banks, and electric vehicles, are significantly cheaper than the prismatic and pouch style batteries that are more commonly seen in consumer electronics. Additionally, they provide substantial capacities, while only occupying slightly more volume. Using the two cells, a capacity of 6000*mAh* is achieved. While this is substantially more capacity than was required, it gives plenty of room to accommodate efficiency losses in the board power supplies, as well as the gradual losses in capacity as the battery is charged and discharged. Additionally, by using these cells, future designs can be scaled up with minimal design effort to accommodate larger and more powerful sensing missions.

The battery charging circuit presented additional opportunities to prolong the operational lifespan of the device. Charging a lithium ion battery to it's nominal charging voltage, and continued cycling, will eventually lead to a degradation of its capacity. However, by providing charge to slightly below its nominal voltage, substantial gains in number of cycles a battery can withstand before losing significant capacity.

A chemistry specific battery chip implemented into the design. Additional design consideration was given in the selection of the necessary supporting components. Due to the concerns of power loss, additional consideration was given during inductor selection, balancing low parasitic, with increased size and material cost.

The main system on a chip (SoC) used required a typical 3.3V input, with an additional 5V rail to power the sensor package. Two buck converter ICs were used to provide the necessary voltage. Similar consideration was used in the selection of the requiset inductor, choosing one with low parasitic, but balanced with regards to the size and cost.

#### B. Power Management

The power received and consumed needs to be managed very efficiently to prolong the lifetime of the sensor network. Energy received from the solar panel is managed using a voltage regulator. The function of this circuit is to provide the proper load to the solar panel to produce the maximum amount of power out of the panel. After this circuit, the power flows into a DC to DC converter to create the necessary voltage to current ratio to properly charge the battery pack. Next, the batteries will be used to power the TI Launchpad. In order to do this, the power will go through a second DC to DC converter in order to supply the proper voltage to the TI Launchpad.

The solar panel will be implemented with a 6V/6W solar panel, the regulator will be implemented with a voltage regulator, the two DC to DC converters will be designed, simulated and tested as a part of this project, and the battery pack will be implemented as two lithium ion batteries.

The voltage regulator will be implemented using a Multimode High-Frequency PWM Controller from Texas Instruments. The model that will be used is the TPS43000. The TPS43000 will be used to operate with a continuous conduction mode (CCM). This will produce 9V to feed to the battery charging circuit.

The battery charging circuit will consist of a DC to DC converter that will step down the 9V from the regulator

to 8.2V in order to charge the batteries. For this project, the batteries that will be used are the Samsung 35E 18650 3500mAh 8A battery. From there, the output voltage of the battery will be stepped down to 3.3V to run the TI Launchpad. The Launchpad will also be responsible for powering the sensors added to the project. Finally, a second DC-DC converter will be implemented to convert the battery source to a 5V supply, which will be used to run the any sensors on the TI Launchpad.

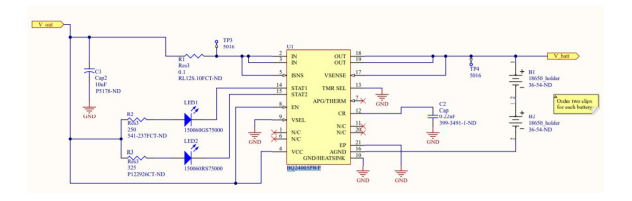


Fig. 9. Schematic of the battery charging circuit

The schematic above shows the circuit that was designed, simulated, and tested to take the 9V input from the voltage regulator and step it down to the 8.2V necessary to charge the battery pack. This designs features the Texas Instruments BQ24005PWP battery charging IC.

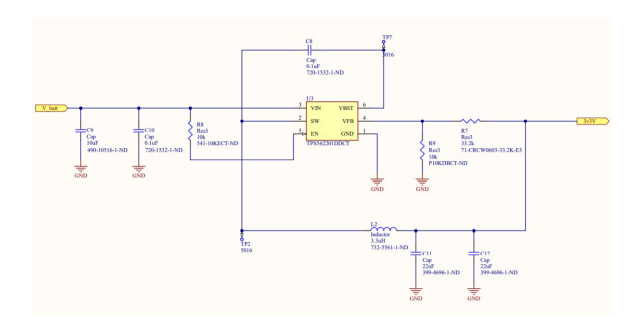


Fig. 10. Schematic of the DC-DC converter to produce the  $3.3\mathrm{V}$  power rail

The schematic above shows the DC-DC converter responsible for converting the output of the battery to a 3.3V source. This 3.3V source will be the source that runs the TI Launchpad as well as any auxiliary sensors not using the 5V rail.

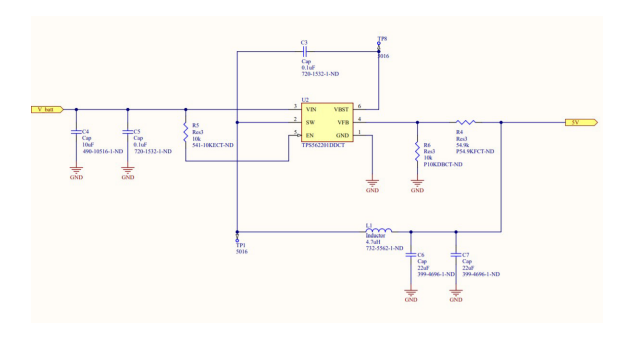


Fig. 11. Schematic of the DC-DC converter to produce the 5V power rail

This schematic shows the final DC-DC converter circuit. This circuit will produce a constant 5V supply to the TI Launchpad to power the main sensors.

## IV. CONCLUSION

While the current star configuration of the network is functional, improvements could be made by a reconfiguration to an intelligent mesh network, which is part of our ongoing future work. Using the current built-in antenna found on the TI launchpad, the network grid is established at a 250 ft. spacing. Future designs will implement a more efficient and compact antenna, while providing additional range should it be required. The power systems will provide the necessary 1000 mAh to power the launchpad for at least two weeks, assuming no availability of solar power, with a an addition buffer of 5000 mAh for increased flexibility in sensor choice, deployment time, and potential solar power loss. The system will also be robust enough to handle harsh northern winters, with little to no interaction from outside help beyond its initial deployment.

### REFERENCES

- J. P. Walker, G. R. Willgoose and J. D. Kalma, "In situ measurement of soil moisture: a comparison of techniques," in Journal of Hydrology 293 '04, Callaghan, NSW 2308, Australia, pp. 85–99, 2004.
- [2] O. Merlin, J. P. Walker, R. Panciera, R. Young, J. Kalma and E. J. Kim, "Soil Moisture Measurement in Heterogeneous Terrain," in MODSIM 2007 International Congress on Modelling and Simulation, 2007.
- [3] W. R. Belisle, A. Sharma and T. L. Coleman, "An optical reflectance technique for soil moisture measurement. I. Theory, description, and application," in IGARSS '96. 1996 International Geoscience and Remote Sensing Symposium, Lincoln, NE, USA, vol.2, pp. 1315-1319, 1996.
- [4] V. S. Palaparthy, S. Lekshmi, J. John, S. Sarik, M. Sh. Baghini and D. N. Singh, "Soil Moisture Measurement System for DPHP Sensors and In Situ Applications," in Proceedings 4th International Symposium on Electronic System Design, pp. 12–15, 2013.
- Electronic System Design, pp. 12–15, 2013.
  [5] O. Calla, D. Bohra, R. Vyas, B. Purohit, R. Prasher, A. Loomba and N. Kumar, "Measurement of soil moisture using microwave radiometer," in 2008 International Conference on Recent Advances in Microwave Theory and Applications, Jaipur, pp. 621-624, 2008.
- [6] C. K. Sahu and P. Behera, "A low cost smart irrigation control system," in 2015 2nd International Conference on Electronics and Communication Systems (ICECS), Coimbatore, pp. 1146-1152, 2015.
- [7] G.J. Gaskin and J.D. Miller, "Measurement of soil water content using a simplified impedance measuring technique," in Journal of Agricultural Engineering Research 63, pp. 153-160, 1996.
- [8] A. Fares, H. Hamdhani and D. M. Jenkias, "Temperature-Dependent sealed frequency: Improved accuracy of multisensory capacitance probes," in Soil Science Society of America Journal, Vol-71, pp. 894-900, 2007.
- [9] E. Veldkamp and J. J. O'Brien, "Calibration of a Frequency Domain Reflectometry Sensor for Humid Tropical Soils of Volcanic Origin," in Soil Science Society of America Journal, Vol. 64, No. 5, pp. 1549-1553, 2000.
- [10] W. Kunzler, S. G. Calvert and M. Laylor, "Measuring Humidity and Moisture with Fiber Optic Sensors," in Proceedings of Sixth Pacific Northwest Fiber Optic Sensor Workshop (SPIE), Vol. 5278, 2003.
- [11] S. K. Khijwania, K. L. Srinivasanb and J. P. Singha, "An evanescent-wave optical fiber relative humidity sensor with enhanced sensitivity," in Journal of Sensors and Actuators B: Chemical, Vol. 104, Issue. 2, pp. 217-222, Jan 2005.
- [12] Sh. Muto, A. Fukasawa, T. Ogawa, M. Morisawa and Hiroshi Ito, "Optical Detection of Moisture in Air and in Soil Using Dye-Doped Plastic Fibers," in Japanese Journal of Applied Physics, pp. L1023-L1025, 1990.
- [13] T. Seiyama, N. Yamazoe, H. Arai, "Ceramic Humidity Sensors', in IEEE Transactions on Components Hybrids, and Manufacturing Technology," Vol. 3 Issue. 2, pp. 85-96, Jun 1980.
- Technology," Vol. 3 Issue. 2, pp. 85-96, Jun 1980.

  [14] I. F. Long and B. K. French, "Measurement of soil moisture in the field by neutron moderation," in Journal of Soil Science, Vol. 18, pp.149–166, 2006.
- [15] D. M. Pozar, 2012. Microwave Engineering. 4th ed. Hoboken, NJ: John Wiley.
- [16] Texas Instruments, 2016. CC-Antenna-DK2 Quick Start Guide. [on-line] Texas Instruments.
- [17] Texas Instruments, 2017. CC-Antenna-Dk2 and Antenna Measurements Summary. Texas Instruments.